



A SCHEMATIC DESIGN OF PIEZOELECTRIC MATERIAL SUBJECTED HORVESTER SURFACE SUBJECTED TO STATIC LOADS

BATTINI NAVEEN KUMAR

M.TECH (Machine Design)
Sana Engineering College
Kodad
bnaveen329@gmail.com

M.SALAR BAIG

Assistant Professor
Sana Engineering College
Kodad
salarbaigm@gmail.com

ABSTRACT:

Piezoelectric vitality collector rummages mechanical vibrations and creates power. Specialists have strived to advance the electromechanical structures and to outline fundamental outside power administration circuits, expecting to convey high control and amended yields prepared for filling in as batteries. Complex misshaping of the mechanical structure brings about charges with inverse polarities showing up on same surface, prompting current misfortune in the connected metal terminal. Outside power administration circuits, for example, rectifiers contain diodes that devour control and have undesirable forward predisposition. To address the above issues, we devise a novel incorporated piezoelectric vitality collecting gadget that is organized by stacking a layer of quantum dabs (QDs) and a layer of piezoelectric material. We find that the QD can redress electrical charges produced from the piezoelectric material in view of its versatile conductance to the electrochemical possibilities of the two sides of the QDs layer, with the goal that electrical current causing vitality misfortune on a similar surface of the piezoelectric material can be limited. The QDs layer can possibly supplant outer correction circuits giving a considerably more conservative and less power-utilization arrangement.

CHAPTER-1

INTRODUCTION

Piezoelectric impact is shown in precious stones with no focal point of symmetry. Under an outside anxiety, a net polarization shows up on the surface of the material, creating piezoelectric voltage, initiating electrical charges. Mechanical-to-electrical vitality reaping gadgets in light of piezoelectric materials have been getting much consideration in late decades.¹²³

Moreover it has been effectively cutting-edge to nanoscale vitality gadgets recently.⁴⁵ Note that charge must be persistently created when there is an adjustment in the connected power, which implies that a static power just creates a settled sum charges that will spill away rapidly over the outside circuit (interior screening impact is disregarded). The time taken for releasing without end all created charges relies upon the information impedance of the outside circuit.

1.1 MODELS AND METHODS:

The multiphysical treatment for this new idea is part into three stages, in particular mechanical-to-electrical (MTE), charge-to-electrochemical potential (CTE), and flexible burrowing (ET) through the quantum dab. Euler-Bernoulli bar hypothesis together with the constitutive piezoelectric condition will be utilized as a part of the MTE organize, CTE recreation depends on semiconductor material science, and ET reproduction is based on the quantum mechanics hypothesis. This open-circle multi-material science recreation connects the outside connected mechanical excitation to the conductance of the QD, through which the amending capacity of this idea is illustrated. At last this incorporated gadget is associated with a heap resistor for showing in the genuine applications.

1.2 CHARGES TO ELECTROCHEMICAL POTENTIAL:

After obtaining piezoelectrically generated



charges, electrochemical potentials (top and bottom surface) of the piezoelectric layer can be derived from the carrier density equation³⁰, which is where $D_3(E)$ is the thickness of state for 3-dimensional mass materials, which appears as $1/32$ where m_0 is the uncovered electron mass $9.11 \times 10^{-31} \text{ Kg}$. n is the transporter thickness, which is endless supply of the piezoelectric cantilever. The extra transporter thickness is ascertained by $\Delta n = Q(t)/(wLdp)$, dp indicates the exhaustion thickness on the surface of the piezoelectric, which can be approximated by the Poisson condition $d^2\phi(z)/dz^2 = e\Delta n/\epsilon_s$. Here for effortlessness it is taken as a consistent 10 nm . $f_0(E)$ is the Fermi dispersion of electrons $1/\exp((E - \mu)/kBT) + 1$, where E is the electron vitality, μ remains for the compound potential, kB is the Boltzmann steady ($8.62 \times 10^{-5} \text{ eV/K}$), and T means the temperature. Emphasis technique/self-predictable strategy is utilized to acquire μ through the numerical approach³³. In the work we figure the Fermi dispersions of electrons in conduction band f_e and openings in valence band f_h , where the electrochemical possibilities μ_e and μ_h are electrochemical possibilities for electrons and openings individually. Reapers can be utilized as battery rechargers in different situations, for example, enterprises, houses the military (with respect to unmanned elevated vehicles and handheld or wearable devices]. The likelihood to abstain from supplanting depleted batteries is exceptionally alluring for remote systems (Wireless Sensor Networks in which the support costs because of battery check and substitution are pertinent. Another developing field of use is biomedical frameworks, where the vitality could be reaped from an off-the-rack piezoelectric unit and used to execute sedate conveyance frameworks or material sensors. Recent inquire about additionally incorporates

vitality change from the occlusal contact amid biting by methods for a piezoelectric layer and from heart thumps. We can arrange the fundamental vitality gathering advances by the pecking order appeared in Figure 1. Movement collector frameworks can be organized as takes after: the gatherer gathers contributions through its casing, straightforwardly associated with the facilitating structure and to the transducer; toward the finish of the framework chain, a molding circuit controls the electrical signs. This paper particularly concentrates on piezoelectric movement reaping strategies.

1.3 TRANSDUCTION PRINCIPLE :

The piezoelectric impact changes over mechanical strain into electric current or voltage. It depends on the key structure of a precious stone cross section. Certain crystalline structures have an accuse adjust of negative and positive polarization, which kill along the nonexistent polar pivot. At the point when this charge balance is annoyed with outer anxiety onto the gem work, the vitality is exchanged by electric charge bearers making a current in the gem. On the other hand, with the piezoelectric impact an outer charge information will make an unbalance in the unbiased charge state causing mechanical anxiety. The association amongst piezoelectricity and gem symmetry are firmly settled. The piezoelectric impact is seen in gems without focus of symmetry, and the relationship can be clarified with monocrystal and polycrystalline structures. In a monocrystal (Figure 3) the polar tomahawks of the greater part of the charge bearers show one-way directional attributes. These gems exhibit symmetry, where the polar tomahawks all through the precious stone would lie unidirectional regardless of the possibility that it was part into pieces.

1.4 VIBRATION-BASED ENERGY HARVESTING

Low-level mechanical vibrations happen

much of the time in conditions, for example, apparatus and vehicles (e.g., a car or air ship). Vibration vitality gatherers are intended to change over encompassing vibrations into power. These gadgets can be separated into two gatherings Non-thunderous and full vitality collectors (i.e., gadget reverberation recurrence is coordinated to vibration include recurrence). A non-full vitality gatherer is more effective where the info contains low frequencies (< 10 Hz), and sporadic vibrations with amplitudes bigger than the device's basic measurements.

CHAPTER-II

LITARATURE

REVIEW

Azzouz et al. (2001), have built up a triangular piezoelectric shallow shell component for breaking down structures with MFC/AFC actuators and thought about the execution of the MFC actuator with 13 that of the conventional PZT actuator. Created component was utilized to explore the impact of PZT fiber introduction on acoustic and basic vibration control of plate and shells. Wang et al.(2001), examined the vibration control of brilliant piezoelectric composite plates and the impact of the extending twisting coupling of the piezoelectric sensor/actuator matches on the framework dependability of savvy composite plates. In light of first-arrange shear hypothesis and steady approach, a brilliant isoparametric limited component was planned and the established negative speed input control technique is received for the dynamic vibration control investigation of keen composite plates with reinforced or inserted conveyed piezoelectric sensors and actuators. proposed the mechanics for the coupled investigation of piezolaminated plate and piezolaminated curvilinear shell structures and their vibration control execution. A plate/shell structure with thin PZT piezoceramic layers inserted to finish

everything and base surfaces to go about as circulated sensor and actuator was considered. introduced another limited component plan for the arrangement of electromechanical limit esteem issues. Instead of the standard definition that utilizations scalar electric potential as nodal factors, this new detailing executes a vector potential from which segments of electric removal are inferred. **Bernadou and Christophe (2003)**,built up a two-dimensional modelization of piezoelectric thin shells the estimation of the second detailing by an accommodating limited component technique was broke down. Singh et al. (2003), depicted Some effective methodologies for the dynamic control of vibrations of a pillar structure utilizing piezoelectric materials. The control calculations have been actualized for a cantilever shaft show created utilizing limited component definition. Lee and Yao (2003), tentatively concentrated the dynamic vibration control of structures subject to outer excitations utilizing piezoelectric sensors and actuators. A just bolstered plate and a bended board were utilized as the structures in tests. The Independent Modal Space Control (IMSC) approach was utilized for the controller outline. Raja et al. (2004), displayed a coupled piezoelectric field with a development strain in the numerical detailing to dissect piezohydrothermoelastic overlaid plates and shells. Limited component actuator and sensor conditions are inferred utilizing a nine-noded field predictable shallow shell component. **Robaldo et al. (2006)**,introduced limited component for the dynamic investigation of overlaid plates implanting piezoelectric layers in view of the rule of virtual relocations (PVD) and a bound together definition. The full coupling between the electric and mechanical fields was considered. Numerical outcomes have been given by them for the free-vibrations

frequencies of essentially upheld plates inserting piezoelectric layers. displayed detailing of a nine-noded piezolaminated deteriorated shell limited component for demonstrating and investigation of multilayer composite general shell structures with reinforced/installed disseminated piezoelectric sensors and actuators. built up a piezoelectric multi-lamina shell FE to display for thin walled structures with piezoelectric fiber composites spellbound with interdigitated terminals (PFCPIE). Another plan for the introduction of the electric field was exhibited. Ivelin V. Ivanov (2011), displayed Active Fiber Composites (AFC) by piezo-electric Finite Elements (FEs) and their successful properties are dictated by FE examination. Dynamic conduct of a shrewd composite structure was reproduced by them in Finite Element. were among the first to exhibit the vibration control methodology for the vast adaptable basic frameworks displayed the assembled or restricted interconnection idea for basic vibration control with circulated actuators and sensors. **Jha and Inman (2003)**, modeled the dynamics of a lightweight, inflatable shell structure commonly used in telecommunications satellites and other space-based structures and also experimentally investigated the suitability of using the MFC for structural vibration applications. **Williams et al. (2004)**, investigated the mechanical properties of the MFC using the classical lamination theory. Nonlinear mechanical behaviors of the MFC were studied by the experiment, and the linear mechanical properties of the MFC were compared with the result of the analytical method. In addition, Williams measured the nonlinear actuation properties of the MFC under various loads. There are also some researches for the application of the MFC to the structure. Ruggerio et al. (2004), used several MFCs as both actuators and sensors to measure the dynamic

behavior of the inflatable satellite structure and to control its vibration. The flexibility of the MFC made for convenient attachment to the doubly-curved surface, and it was found that MFC outperformed the other actuators. used the flexibility and high force output of the MFC to snap-through an unsymmetric composite laminate from one stable configuration to the other. demonstrated experimentally the application of MFC actuators in vibration control of aluminum beam and metal music plate. The MFC'S are used, one as an exciter and other as an actuator. ANSYS was used to model the structures with thermal analogy for including the piezoelectric actuation. adopted a LQR based feedback control strategy using MFC actuators to suppress the flexural vibration of cycle handle bar to establish the natural frequencies and mode shapes. **Shon and Choi (2008)**, utilized GA to ideally put MFC actuators on tube shaped aluminum shell and led dynamic vibration control tests. A Lagrangion based hypothetical detailing was made by them to catch the elements of the shell including the electro-mechanical couplings of MFC actuators performed hypothetical and test examinations on aluminum barrel shaped shell vibration control utilizing the MFC actuators. The hypothetical model was produced by them utilizing Rayleigh Ritz estimation and the strain dislodge relations are set up in view of Donnel-Mushtari hypothesis. Initial three methods of the barrel are effectively controlled by an uplifting position criticism, actualized in DS1104. Rolf actualized Piezoelectric full scale fiber composites (MFCs) actuators into a dynamic composite wing. Dynamic tests were additionally performed by them on a sandwich wing of a similar size with customary aileron control for correlation.

CHAPTER 3

METHODOLOGY

3.1.2 Electrical Systems:

CATIA offers an answer for encourage the plan and assembling of electrical frameworks dispersal over the entire procedure from reasonable outline through to producing. Capacities incorporate prerequisites catch, electrical schematic definition intuitive 3D steering of both wire bridles and modern link arrangements through to the creation of point by point producing records counting formboards.

3.2 ENERGY HARVESTING: MODELLING FRAMEWORK:

For the forecast of the vitality reaping capacities of a piezoelectric film joined to the surface of the wing, a FE was created in ANSYS 13.0 (ANSYS Inc. Canonsburg, PA, USA). The strong model is a 3-mm thick substrate a piezoelectric film connected at its middle. The substrate is an area wing made of HexPly 3501-6 epoxy network and strands composite having the format [(46/86/ - 42/0)4], as acquired from the past wing streamlining. The properties the cured overlay employs are given in Table 2. It was accepted that the PZT film was attached to the composite substrate a basic epoxy cement (DP460 from 3M, pertinent properties in Table 3) of thickness chose inside the range to 50 μm . The piezoelectric material picked is PZT-5H (properties in Table 4) for its great vitality era. A scope of estimations of thickness was, from 10 to 200 μm , and in addition a scope of side lengths from mm^2 to $10 \times 10 \text{ mm}^2$. Normally, a genuine reaper settled to the wing could be considerably bigger; the upper esteem investigated this work was managed by the computational cost of recreation. Misusing the symmetry of the setup, just 1/4 the geometry was really demonstrated with FE; parameters showed in the accompanying and the outcomes announced are for the full gadget. The substrate was coincided with Layered Solid

components, the epoxy cement with Structural components and the PZT film with Piezoelectric Solid components, which have electrical and mechanical, allowing the displaying of the piezoelectric impact in a multi-material science show. Anodes were characterized on the sides of the piezoelectric film, by coupling the voltage DoF of the hubs, and associated with a Circuit component as a resistor whose esteem was made to differ to investigate its impact on control yield. The stacking information was to the composite substrate as a removal imperative at the edges, in order to create inside the substrate the - subordinate strain motion on the wing (Figure 3). In of the way that information in Figures 1 and 2 are for an blast ($V=17.6 \text{ m/s}$) and that the strain is not uniform over the wing surface, for the power forecast count pinnacle strain was thought to be just 1300 μstrain , i.e. the info strain waveforms to the FE display were roughly 1/3 of those in the below table.

Mechanical properties (HexPly® 3501-6 AS4)	
Young's modulus (long.)	142 GPa
Young's modulus (transv.)	10.3 GPa
Poisson's ratio	0.27
In-plane shear modulus	7.2 GPa

3.3 PIEZOELECTRIC ENERGY HARVESTING MODELS

Coupled electromechanical models of piezoelectric materials are inferred for and execution investigation of vitality collectors. Utilizing the 1-D design in figure the constitutive relations can be streamlined as

Drag compel Drag should likewise be considered when planning our air cushion vehicle. Accepting that our outline creates enough lift to basically make the surface frictionless, drag is the main power that contradicts the air cushion vehicle's forward

movement. Be that as it may, we can diminish this power. The drag is caused when the air cushion vehicle travels through a liquid, for example, air. The drag power can be figured utilizing the accompanying condition: $F_d = 1/2 * \rho v^2 C_d A$

Where, ρ is the thickness of the liquid, v is the speed of the air cushion vehicle with respect to the liquid, A is the cross-sectional range of the air cushion vehicle, C_d is the coefficient of drag. The coefficient of drag is a unit-less proportion between the drag drive and the dynamic weight times the range. This coefficient is normally found through analysis and can be computed through the condition: $C_d = F_d / \rho A v^2 / 2$

In Figure the drag co-efficient for different shapes was given. From these conditions, we can verify that drag must be considered when planning the air cushion vehicle's body shape and size. We will likely influence our air cushion vehicle to outline more streamlined by diminishing the cross-sectional range of the reference confront and wiping out any level surfaces opposite to the stream of air. Choosing a streamlined plan with a more slender last part will diminish the wake created by our air cushion vehicle. A littler wake implies less drag created and in this way, brings down contradicting powers, bringing about a speedier air cushion vehicle. Since, according to the measurements our air cushion vehicle is a short chamber, the C_d can be taken as 0.82.

$$F_d = 1/2 * \rho v^2 C_d A$$

$$F_d = 0.5 * 1.225 * 15 * 15 * 0.82 * 5$$

$$F_d = 40.18 \text{ kN}$$

Accordingly, Drag compel following up on the Hovercraft is 2.4653 N that power additionally called as erosion drive. A drag compel follow up on the Hovercraft is constantly negative. Clark Y Airfoil The airfoil has a thickness of 11.7 percent and is level on the lower surface from 30 percent of harmony back. The level base streamlines

point estimations on propellers, and makes for simple development of wings on a level surface. The airfoil area is appeared in Figure 3. It gives sensible general execution in regard of its lift-to-drag proportion, and has delicate and moderately considerate slow down attributes. Computer aided design Model The Clark Y airfoil arranges are transported in and created as a 3D display with the traverse of 1 m appeared in underneath Figure. The base structure of air cushion vehicle SKIMA 4 with Clark Y airfoil wing was displayed utilizing CATIA with measurements of 4*1.5 m² is appeared in underneath Figure. Add up to vitality gathered from the EH as an element of the electrical load. This plot is for the 5x5 mm², 100- μ m thick PZT fortified with 5 μ m of cement and subject to the 5 Hz blast.

3.4 DYNAMIC MODELING OF A ROTATING CANTILEVER BEAM WITH PIEZOELECTRIC ELEMENT:

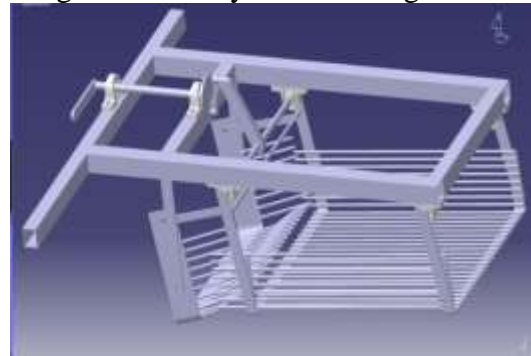
We infer a scientific model of the vitality gatherer that mechanical diversions, center point speed, and different parameters with the produced charge. To this end, the coupled dynamic model of a pivoting adaptable shaft is and incorporated with electrical circuit conditions in light of the impact of transducer. Conditions are illuminated to remove shut frame articulations for reaction and electrical yield of the framework. Impact of various parameters on collector flow investigated in this part. The parameters incorporate shaft length, mass, damping and piezoelectric material properties, for example, piezoelectric consistent, and relative allowing. Add up to vitality delivered by the EH as an element of PZT thickness. The span of the PZT is 5x5 mm² and the thickness of the is 5 μ m. Information are ascertained at their own particular ideal estimation of electrical load.

3.5 VITALITY HARVESTING: MODELING DISCUSSION

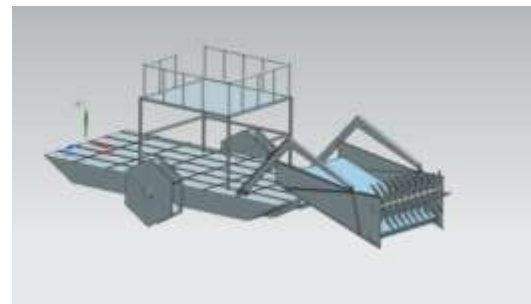
As depicted some time recently, the zone vitality thickness is not steady but rather increments with the PZT measurements; additionally, the aggregate vitality with the thickness of the PZT, yet not as quick as a straight reliance would anticipate; at long last, thicker layers of glue cause a decreased vitality era. Every one of these wonders can be clarified by the proficiency with which the mechanical strain in the composite substrate is exchanged to the PZT layer. As the PZT ends up plainly thicker, bigger powers are expected to completely strain it; as the coupling amongst substrate and PZT is given by the glue, its limited (as contradicted to interminable) solidness sets a few cutoff points. The expansion of territory vitality thickness in bigger PZT films is clarified by Figure. there is an edge impact whereby the best and base areas of the PZT are not subject to the full strain experienced by the rest of the material. The measure of the locales influenced by bring down strain levels is dictated by the thickness of the PZT instead of its size, so that in a bigger gatherer they are relatively littler and cause a littler loss of effectiveness. The yield impedance of the gatherers demonstrated is fairly high, in overabundance of 25 M ω for the 5x5 mm² 100 μ m-thick gadget. While these qualities are unrealistic, as the power administration unit ought to have a coordinating information impedance, they are because of the little measurements that could for all intents and purposes be displayed. A practical collector put on a flying machine wing would be no less than 100x100 mm², diminishing the ideal electrical load to just several k ω .



Figure 3.2 safety factors along X-axis



3.3 schematic design of harvester using CATIA



3.4 isometric view of Harvester using CATIA

CHAPTER-IV

RESULTS

A contextual investigation to quantitatively exhibit this thought is nitty gritty in this area. The numerical methodology starts with the mechanical examination. In unraveling the condition (1), the sufficiency of periodical main impetus A_n is set to $m_t a$ where m_t is the total of the cantilever mass and the confirmation mass, an indicates the remotely connected speeding up (10 m/s²). The straight firmness of the cantilever can be computed from $k_1 = (Y w g^3) / (4 L^3)$ 39, nonlinear solidness $k_2 = 2 k_1$, and the

damping factor is more often than not small for scaled down gadgets. Here we utilize $b = 2(kl/mt)^{1/2} \times 10^{-5}$. From the numerical arrangement of the condition (1), substitute tip avoidance $z(t)$ into the conditions (2)-(4), created charge $Q(t)$ is computed as for time t . Figure 2 delineates the aftereffect of $z(t)$ and $Q(t)$. It is seen that the cantilever wavers occasionally with a greatest pinnacle dislodging of $1.1\mu m$, created charge wavering in a comparable way with the pinnacle abundance of $3.66 \times 10^{-12} C$. Next the subsequent charge esteems are contribution to the condition (5) to touch base at concoction possibilities μ_e and μ_h , which are mapped to the band chart furthermore, demonstrated together with μ_c and μ_v in Figure 3. It is seen from Figure 3a that in the low thickness go, a little expansion of the bearer thickness makes compound potential go amiss to μ_c or μ_v quickly. Yet, the concoction potential stays consistent in the expansive thickness run. That is because of the exponential idea of the Fermi-Dirac conveyance of electrons in both conduction what's more, valence groups. As the cantilever vibrates, the concoction potential on the best side of the piezoelectric layer (joining to the QDs) μ_P regarding time t is appeared in the Figure 3b. Contrasted and the outcomes in Figure 2b, μ_P bend shows a square wave rather than a sinusoidal, which matches with the consequences of μ_e and μ_h versus bearer thickness. Promote on, the electrochemical potential μ_P is utilized to compute the condition (8) with the end goal of getting conductance as the capacity of time t . Conductance $G(t)$ is then acquired numerically for a solitary quantum spot. Assume specks thickness is $2.78 \times 10^{14} m^{-2}$, add up to conductance of the entire surface region of the cantilever G_t can be thought to be the whole of many single conductances G_0 associated in parallel. At that point it is $G_t = \sum G_0 = 6.94 \times 10^8 G_0$.

The outcomes are appeared in the Figure 4, where both $R(t)$ (resistance) and conductance $G(t)$ bends are shown. Conductance shifts from a low esteem ($1.74 \times 10^{-8} S$) to a high esteem ($0.07 S$), comparing to resistance from $5.74 \times 10^7 \omega$ to 14.5ω . A straightforward circuit comprising of the coordinated gadget what's more, a $1 k\omega$ resistor is portrayed to exhibit the amendment impact. From Figure 5, plainly the correction impact has been accomplished and all positive piece of the voltages has been obstructed because of huge impedance of the QDs layer, credited to its vitality choice component, where V_1 and V_2 allude to the proportionate circuit in Figure 1c. Graphical exhibit of conductance versus synthetic potential ($G-\mu_P$) bend with the differing δz for a solitary QD is appeared in Figure 6, which obviously shows an execution like that of diodes. As the present courses through the nearby circle circuit comprising of a limited outer load resistance, the electrochemical potential μ_P movements to the nonpartisan. Results from condition (5) (Figure 3b) uncovers that the variety of the μ_P is fundamentally dictated by the extremity of the aggregated charges in the QD-Piezoelectric interface. A little amount of charges will bring the μ_P near μ_c or μ_v , and additionally expanding the amount does not change μ_P altogether (Figure 3a). This makes the metal-QD-piezoelectric interface as an impeccable rectifier contrasted with the exemplary diodes that require a forward inclination. Complex movements of the mechanical structure give accuses of inverse signs on the a similar surface, for illustration a third resounding mode showed in Figure 7. The mode shape is acquired from Euler-Bernoulli pillar hypothesis on cantilever resonance⁴⁰, the third resounding mode is found by numerically illuminating the third root β_3 of the nonlinear condition $\cosh(\beta_n L) \cos(\beta_n L) + 1 = 0$. dz^2/dx^2 is for the

bend at x purpose of the cantilever. Thusly the mode shape and charge appropriation can be ascertained. It is seen that both positive and negative charges are created at first glance, causing charges cancelation. With the QDs layer, just a single sort of charges can course through, lessening the present misfortune on cathode.

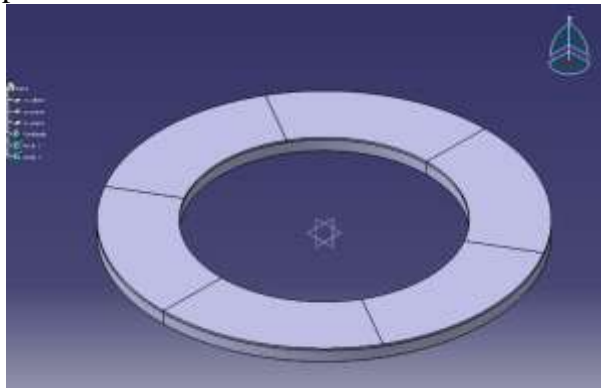


Figure 4.1 Piezoelectric Materials used For Harvest Surface

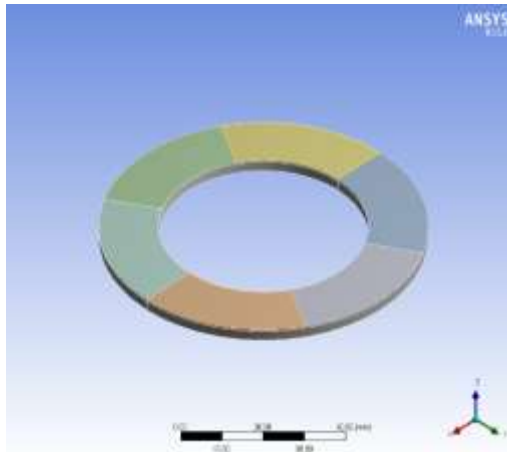


Figure 4.3 Piezoelectric Surface Material Various Stress

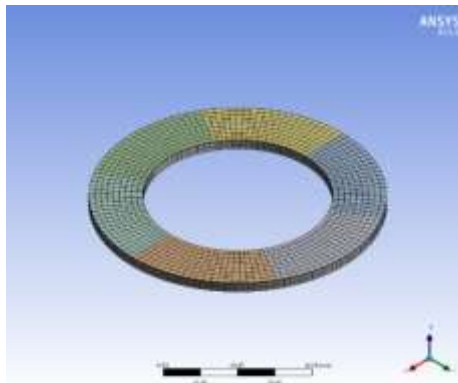


Figure 4.4 Meshing Model Of The Piezoelectric Surface Material

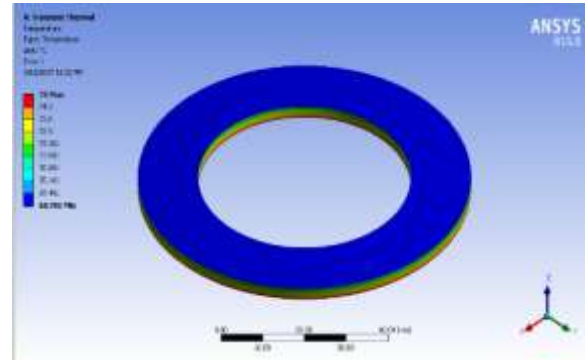


Figure 4.5 piezoelectric Surface Material Elastic Stress

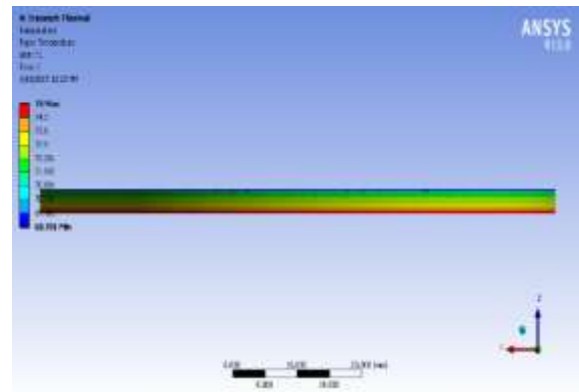
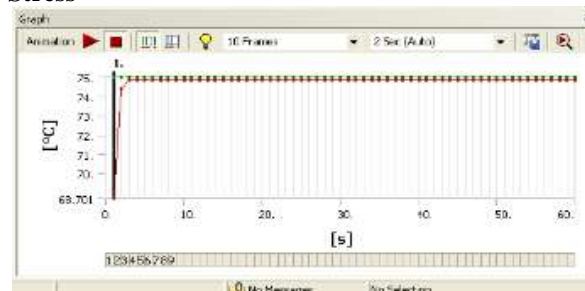
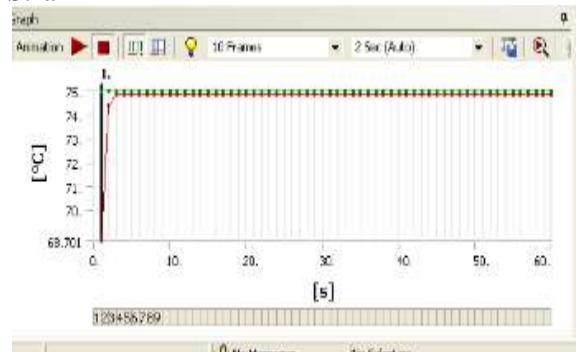


Figure 4.6 piezoelectric Surface Material Elastic Strain



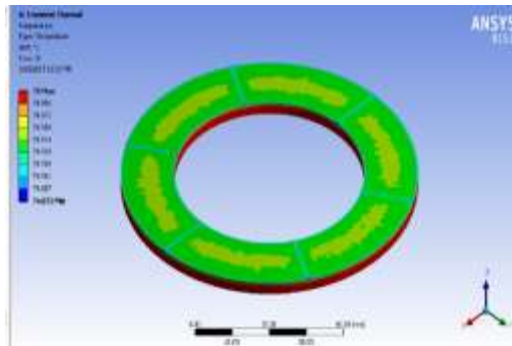


Figure 4.6 piezoelectric Surface Material Equivalent Elastic Strain

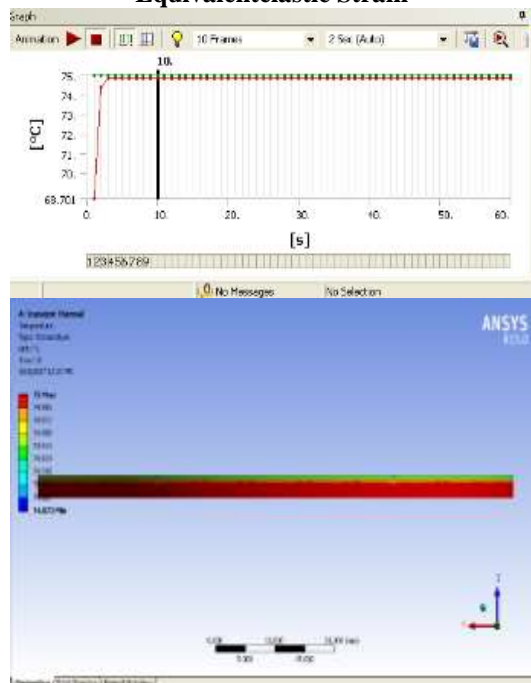


Figure 4.7 Piezoelectric Surface Material Elastic Stress

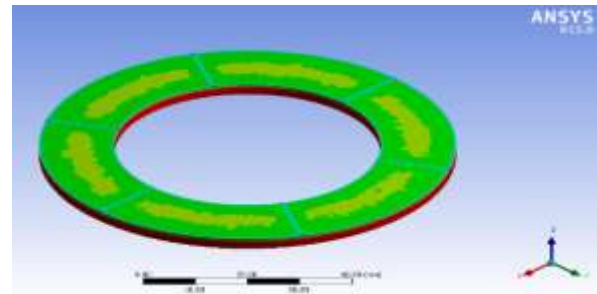
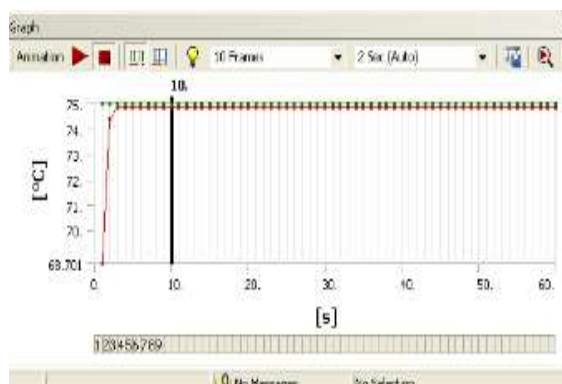
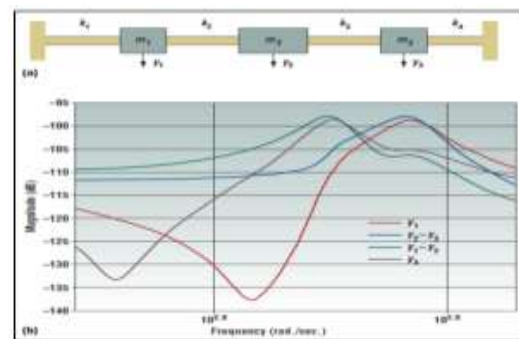
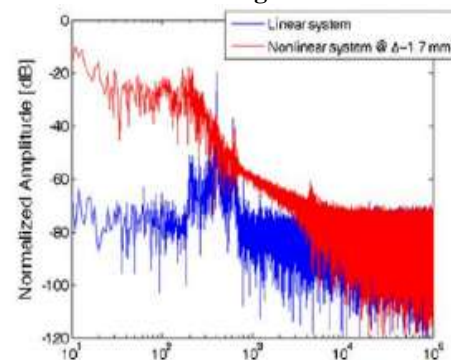


Figure 4.8 piezoelectric Surface Material Total Deformation



4.1 Graph Piezoelectric Surface Material Discharge



4.1 Graph Piezoelectric Surface Material Stress Variations

CHAPTER-5

CONCLUSIONS

With the general point of lessening airplane weight and support cost, a weight-streamlined wing structure was gotten and piezo-reapers were assessed as vitality supply for remote sensor hubs in flying machine auxiliary wellbeing checking. Time-area strain waveforms were figured for the wing skin when the air ship was

subjected to blast stacking. While whirlwinds frequencies (5 and 10 Hz) instigate a maintained vibration of the wing, slower blasts (1 and 2 Hz) create a semi-static diversion of the wing. A parametric report was completed, which demonstrated that expansive and thin PZT gatherers are to be favored for vitality era effectiveness: in a vast PZT collector, edge impacts that antagonistically influence vitality proficiency are less imperative; thin reapers are all the more proficiently coupled to the substrate. Additionally, thin layers of glue are favored for their expanded solidness and adequacy in mechanically coupling collector to substrate. In this work, the PZT collector was subjected to a strain of up to 1300 μ strain, which is inside the points of confinement endured by mass PZT materials for a substantial number of cycles. An option might be spoken to by the utilization of cutting edge composite piezoelectric materials like Micro Fiber Composites, which are relied upon to withstand strains of around 2500 μ strain, yielding a potential 4-overlay increment in vitality era. One preferred standpoint of this vitality gathering approach is that vitality is created additionally amid navigating and amid long flights. The most engaging element of this vitality gathering arrangement is the position of safety of the gatherer (the PZT film thickness is just 100 μ m, a MFC is a couple of tenths of a millimeter thick), its low obtrusiveness and weight. Future works should take a gander at the measurable occurrence of whirlwinds frequencies and amplitudes to evaluate the normal power delivered amid a run of the mill flight.

REFERENCES:

2. Samson, D., Kluge, M., Becker, T. what's more, Schmid, U., "Remote Sensor Node Powered via Aircraft Specific Thermoelectric Energy Harvesting," *Sensors and Actuators A: Physical*, 172(1), 240-244 (2011)

3. Churchill, D.L., Hamel, M.J., Townsend, C.P. what's more, Arms, S.W., "Strain Energy Harvesting for Wireless Sensor," in *Proc. SPIE 5055*, 319-327 (2003)

4. Paradiso, J.A. what's more, Starner, T., "Vitality rummaging for versatile and remote gadgets," *IEEE Pervasive Computing*, 18-27 (2005)

5. Zhu, D., Beeby, S.P., Tudor M.J. what's more, Harris N.R., "A charge card measured self controlled brilliant sensor hub," *Sensors and A: Physical*, 169(2), 317-325 (2011)

. Pozzi M. what's more, Zhu M., "Culled piezoelectric bimorphs for knee-joint vitality gathering: displaying and test approval," *Smart Mater Struct.* 2(5): 055007 (2011)

7. Wang J., Callus P. what's more, Banister M. Trial and numerical examination of the strain and pressure of un-indented and scored semi isotropic covers. *Composite Structures* 64, 297-306 (2004)

8. Kim, J.K., Kim, H.S. what's more, Lee D.G., "Grip qualities of carbon/epoxy composites treated with low weight plasmas," *J. Grip Sci. Technol.*, 17(13), 1751– 1771 (2003)

[9]Jansen, A. J. furthermore, Stevels, A. L. N. "Human Power, a Sustainable Option for Gadgets," *Proc. of IEEE Int. Symposium on Electronics and the Environment*, 1999, pp. 215-218.

[10] Donelan, J. M., Li, Q. furthermore, Naing, V., "Biomechanical vitality gathering: Producing power amid strolling with insignificant client exertion" *Science*, 2008, 319(5864):

807– 810.

[11] Mitcheson, P., Stark, B., Miao, P., Yeatman, E., Holmes, An., and Green, T., "Investigation and advancement of MEMS electrostatic on-chip control supply for self- fueling of moderate sensors," *Euroensors, Portugal*, 2003, pp. 48– 51.

[12] Williams, C.B. also, Yates, R.B., "Examination of a Micro-electric Generator for Microsystems" *Sensors and Actuators A*, 1996, 52:8-11.

[13] Meninger, S., Mur-Miranda, J., Lang, J., Chandrakasan, A., Slocum, A., Schmidt, M. also, Amirtharajah, R., "Vibration to electric vitality change" *IEEE Trans Very Huge Scale Integration (VLSI) Syst.*, 2001, (9) 64– 76.



[14] Sterken, T., Fiorini, P., Baert, K., Puers, R. also, Borghs, G., "An Electret- based Electrostatic Micro Generator" *TRANSDUCERS, Solid-State Sensors, Actuators also, Microsystems, twelfth International Conference, Boston, MA, USA, 2003, 1291–1294.*

[15] Beeby, S.P., Tudor, M.J. also, White, N.M., "Vitality Harvesting Vibration Sources for Microsystems Applications" *Meas. Sci. Technol.*, 2006, 17 175-195.